Current Biology 20, 1029–1034, June 8, 2010 ©2010 Elsevier Ltd All rights reserved DOI 10.1016/j.cub.2010.04.017

Report

The Cortical ER Network Limits the Permissive Zone for Actomyosin Ring Assembly

Dan Zhang,[1,2] Aleksandar Vjestica,[1,2] and Snezhana Oliferenko[1,2,*]

[1]Temasek Life Sciences Laboratory, 1 Research Link, 117604 Singapore

[2]Department of Biological Sciences, National University of Singapore, 117543 Singapore

Summary

Precise positioning of the cellular division plane is important for accurate segregation of genetic material and determination of daughter cell fates. Here we report a surprising connection between division site positioning and the organization of the cortical endoplasmic reticulum (ER). The cortical ER is an interconnected network of flat cisternae and highly curved tubules sharing a continuous lumen [1, 2]. Stabilization of high curvature by reticulon and DP1 family proteins contributes to formation of tubules [3–5]. We show that in the fission yeast *Schizosaccharomyces pombe*, the ER network is maintained by a set of three membrane proteins: reticulon/Rtn1p, DP1/Yop1p, and a newly identified evolutionarily conserved protein, Tts1p. Cells lacking the ER domain sustained by these proteins exhibit severe defects in division plane positioning as a result of abnormal dispersion of a key regulator of division site selection, Mid1p, along the cell cortex. This triggers delocalized assembly of actomyosin cables and compromises their compaction into a single medially positioned ring. We propose that the cortical ER network restricts the lateral motion of Mid1p and hence generates a permissive zone for actomyosin ring assembly precisely at the cell equator.

Results and Discussion

The *Schizosaccharomyces pombe* genome encodes one reticulon and one DP1/Yop1 protein, which we term Rtn1p (SPBC31A8.01C) and Yop1p (SPCC830.08C). Rtn1p-GFP predominantly localized to the peripheral (cortical) endoplasmic reticulum (ER) and was largely excluded from the nuclear envelope (NE), consistent with localization in budding yeast [6]. On the other hand, Yop1p-GFP localized to both the peripheral ER and NE (Figure 1A). Interestingly, Rtn1p and Yop1p accumulated at the cell equator during mitosis, following assembly of the actomyosin ring marked by the myosin light chain, Rlc1p (Figure 1A). From a genetic screen for modulators of Cut11p function in spindle pole body anchorage at the NE [7] (unpublished data), we identified an evolutionarily conserved transmembrane protein (SPBC1539.04) with a strikingly similar subcellular distribution. This protein, Tts1p (*tet*ra-spanning protein 1), colocalized with Rtn1p and Yop1p in the peripheral ER and was also found at the NE (Figure 1B). The compartment marked by Tts1p, Rtn1p, and Yop1p was distinct from membranes containing the ER resident protein oligosaccharide-transferase Ost1p (see Figure S1A available online). Tts1p was enriched at the cell equator during mitosis together with Rtn1p and Yop1p, unlike Ost1p and the translocon subunit Sec63p [8] (Figure 1A; data not shown). Thus, the peripheral ER in fission yeast is organized as an intricately compartmentalized network of high-curvature (tubular) and low-curvature (cisternal) elements.

Mass spectrometry analysis of proteins copurified with the TAP-tagged Tts1p identified Rtn1p as a Tts1p-interacting partner (Figure S1B). We confirmed their interaction by dual coimmunoprecipitation (Figure 1C). Furthermore, Rtn1p interacted with Yop1p (Figure S1C), consistent with reports from budding yeast [3]. We also detected an association between Tts1p and Yop1p by coimmunoprecipitation (Figure S1C). Thus, our data suggest that Rtn1p, Yop1p, and Tts1p colocalize in a subcompartment of the ER and physically associate.

We wondered whether Rtn1p, Yop1p, and Tts1p function together in shaping ER membranes. We examined ER morphology with fluorescent markers for different ER compartments in wild-type and mutant genetic backgrounds. In *rtn1*Δ cells, both Yop1p-GFP- and Tts1p-GFP-marked membranes were significantly depleted from the lateral cortex (Figures 2A and 2B), suggesting diminishment of peripheral tubules. Tts1p and Yop1p in *rtn1*Δ cells were still clearly excluded from the cisternal compartment marked by Ost1p (Figure S2A). Consistent with a conversion to more cisternal ER, Ost1p in *rtn1*Δ cells localized extensively along the lateral cortex, unlike its typical intermittent pattern in wild-type cells (Figure S1A).

Similarly, Rtn1p-GFP showed decreased occupancy at the cell cortex in both *yop1*Δ and *tts1*Δ cells, and its occupancy was further diminished in the double *yop1*Δ*tts1*Δ mutant (Figure 2C). We performed similar analyses for other single and double deletions, with Yop1p-GFP (Figure 2A) or Tts1p-GFP (Figure 2B) as markers for the tubular ER. The reduction in occupancy of tubular ER markers was statistically significant in all cases, with double-deletion strains exhibiting augmented phenotypes. This was not due to compromised marker protein expression (Figure S2B). Of the three proteins, Rtn1p had the largest influence on the distribution of putative tubular ER markers.

As compared to the wild-type, the cortical ER domain visualized by Ost1p-mCherry in the triple *tts1*Δ*rtn1*Δ*yop1*Δ mutant cells (subsequently called *try*Δ) was more prominent and continuous, with occasional extended breaks (Figure S2C). To address how the deficiency of Rtn1p, Yop1p, and Tts1p affected general ER structure, we constructed artificial luminal ER markers, GFP-AHDL and mCherry-AHDL. Because the ER possesses a continuous intraluminal space, these markers localized to both cisternal and tubular compartments (Figure S2D). In wild-type cells, the cortical ER appeared as an elaborate and regularly distributed membranous network underlying the plasma membrane (Figure 2D, top; n = 50 cells). We observed that this regular network structure was disrupted in *try*Δ cells: the cortical ER now mostly appeared as continuous sheet-like membranes (Figure 2D, bottom; n = 50 cells). Additionally, we noticed irregular membrane accumulations and occasional breaks at the cortex. Because the geometry

*Correspondence: snejana@tll.org.sg

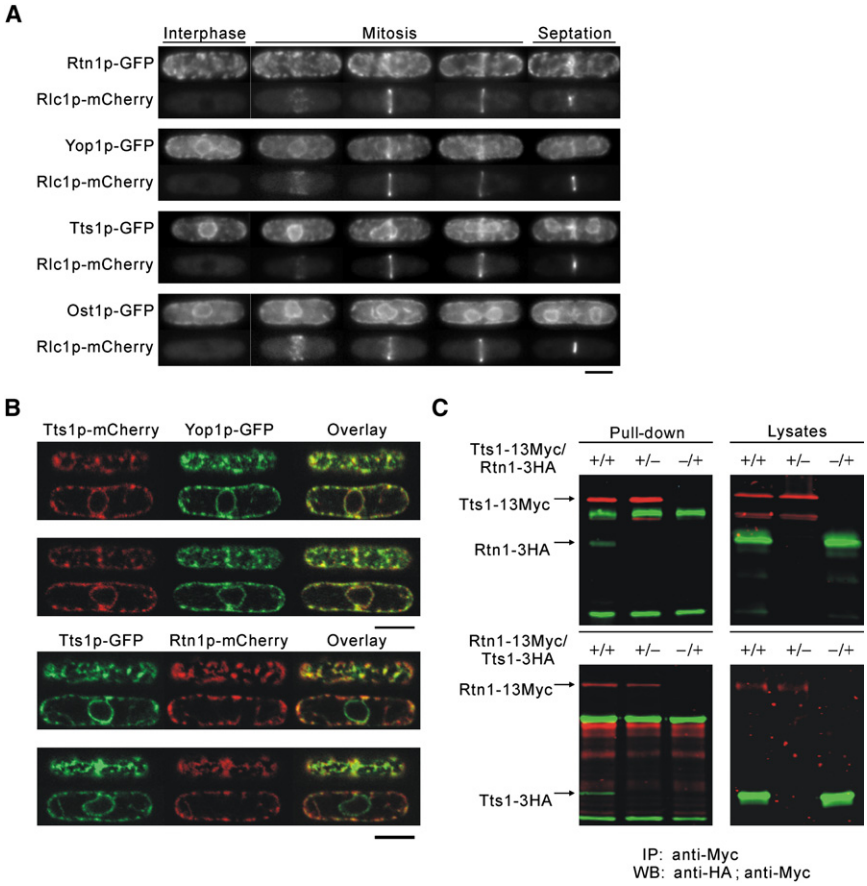

Figure 1. Rtn1p, Yop1p, and Tts1p Colocalize in the Cortical Endoplasmic Reticulum and Accumulate at the Mitotic Cell Equator

(A) Localization of GFP-fused proteins at cell-cycle stages indicated by coexpressed myosin light chain Rlc1p-mCherry as the actomyosin ring marker. Shown are maximum Z projections of epifluorescence micrographs.

(B) Scanning confocal micrographs of cells expressing indicated proteins. Shown are top and middle planes from Z stacks. Scale bars represent 5 μm.

(C) Coimmunoprecipitation of the indicated proteins from native cell extracts. Samples were probed with the anti-Myc (red) and anti-HA (green) antibodies.

of fission yeast cells impedes the resolution of fine details of cortical ER organization, we visualized GFP-AHDL in spheroplasts where the cell wall was removed and cells assumed a spherical shape. This allowed us to clearly document the transition between the intricate ER network in wild-type cells and continuous sheet-like membranes in a *try*Δ genetic background (Figure 2E). Taken together with work in other systems [3], our results indicate that Rtn1p, Yop1p, and Tts1p collaborate to maintain the tubular ER at the cell periphery.

Surprisingly, we observed a progressive failure in division site positioning as cells lost Tts1p, Yop1p, and Rtn1p. *S. pombe* cells position actomyosin rings in the cell center and divide perpendicular to the long axis of the cell. Single mutants for each *try* gene produced a low incidence of tilted and off-center septa. The proportion increased in double and triple mutant combinations. Interestingly, the deficiency of Rtn1p that individually had the strongest effect on ER structure consistently caused a more prominent cytokinesis defect. The triple mutant *try*Δ cells showed the highest incidence of multiple septa and long-axis septa (Figure 3A). The vast majority of *try*Δ cells (92.3% ± 1.8%; n = 1500 cells) failed to normally position septa and resembled cells lacking the anillin-like protein Mid1p that determines actomyosin ring positioning [9–12] (Figures 3A and 3B). Deletion of *mid1* in a *try*Δ genetic background did not exacerbate division site mispositioning, suggesting that Mid1p and the TRY proteins function in the same epistasis group (Figures 3A and 3B). The kinase Pom1p functions as a negative regulator of division site selection [13, 14], and cells lacking both Mid1p and Pom1p were reported as inviable [11]. We obtained mutant cells lacking the *try* genes together with *pom1* at a frequency much lower than expected from tetrad analysis (17% of the expected yield, 88 progeny). The quadruple mutant cells were severely retarded for growth and exhibited extreme septum positioning defects, including frequent tip septa (Figure S3A). This further suggests that the TRY proteins function together with Mid1p in a pathway that is distinct from the Pom1p pathway.

Mid1p shuttles between the nucleus and cell cortex during interphase, but upon entry into mitosis it redistributes to the medial cortex, where it is detectable as distinct nodes [15]. We found that Mid1p-GFP exited normally from the nucleus in triple mutant cells and was recruited to the cortex (Figure 3C, 20 of 23 wild-type and 8 of 10 *try*Δ cells completed Mid1p export within 4 min following spindle pole body [SPB] separation). The total levels of Mid1p-GFP were comparable in wild-type and *try*Δ cells (Figure S3B). Intriguingly, Mid1p spread along a larger area of the cortex and failed to compact into a tight ring (Figure 3C, see kymographs for Mid1p-GFP time evolution). As a result of this abnormal dispersal, the cortical domain occupied by Mid1p was much broader in early mitotic *try*Δ cells as compared to the wild-type (Figure 3D). Notably, we observed that Mid1p-GFP was now largely present in cortical nodes of lower mean fluorescence intensity (Figure S3C; n = 140, p = 0.0013, Kolmogorov-Smirnov test). Unlike wild-type cells that compacted rings during early mitosis, 10 of 15 *try*Δ cells failed to compact Mid1p into rings, and ring formation was strongly delayed in 5 of 15 *try*Δ cells. We did not observe mislocalization of Pom1p, the negative regulator of Mid1p localization, during interphase (Figure S3D).

Given that cortical Mid1p failed to compact into rings in *try*Δ cells, we examined whether it recruited essential ring components such as myosin II and F-actin by using Rlc1p-mCherry and the GFP-tagged Rng2p calponin homology domain as markers. In *try*Δ cells, Rlc1p-mCherry promptly associated with all cortical Mid1p-GFP nodes, as in the wild-type (Figures 3E and 3F; n = 15 cells). Furthermore, actin filaments appeared around the cortical nodes marked by Rlc1p-mCherry in both wild-type and *try*Δ cells (Figures 3G and 3H; n = 20 cells). The timing of actin recruitment to the cortex was not affected (2.5 ± 0.9 min after SPB separation in wild-type, n = 9 cells; 2.9 ± 1.0 min in *try*Δ cells, n = 13 cells; Figure S3E). Thus,

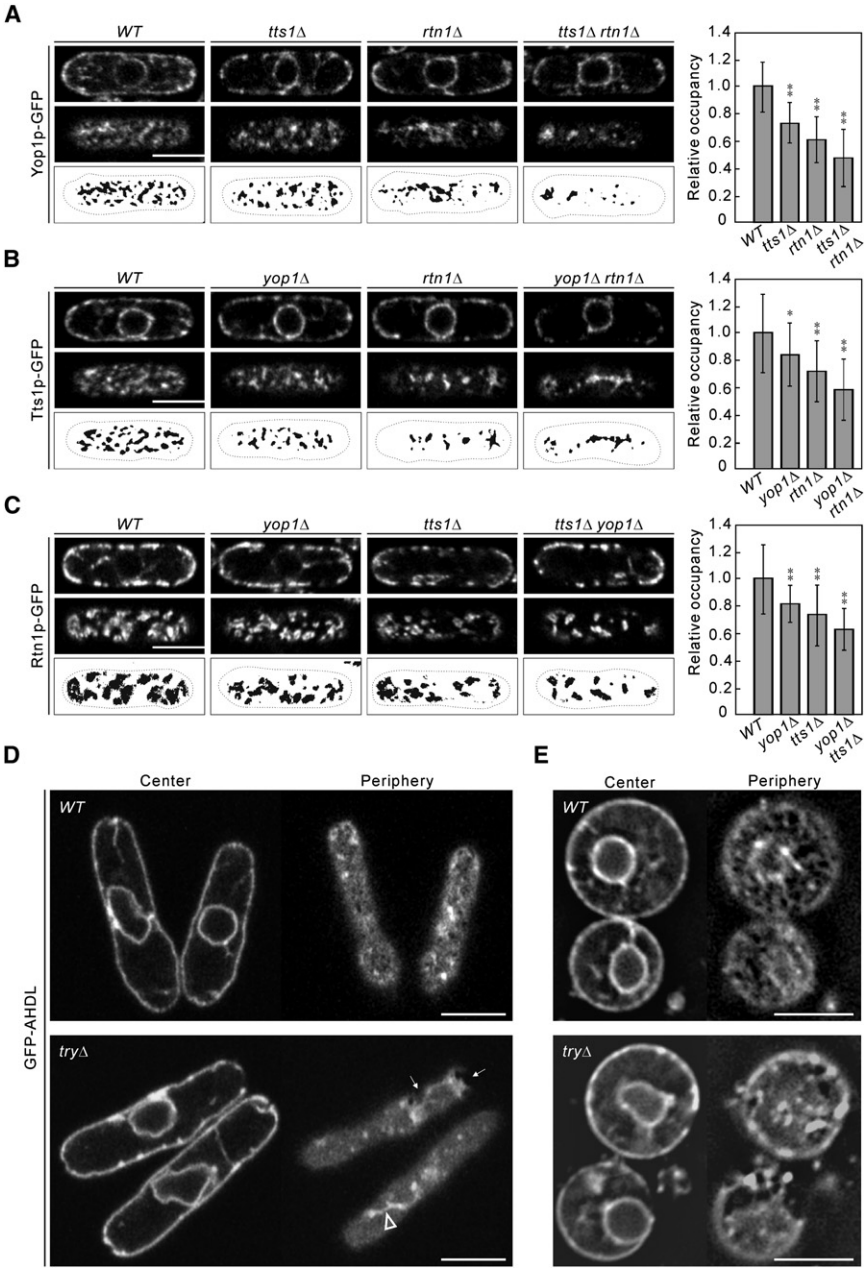

Figure 2. Rtn1p, Yop1p, and Tts1p Maintain the Tubular Structures in the Cortical Endoplasmic Reticulum

(A–C) Scanning confocal micrographs of Yop1p-GFP (A), Tts1p-GFP (B), and Rtn1p-GFP (C) in cells with indicated genetic background. Top: cell center; middle: cell periphery; bottom: thresholded image of cell periphery. Histograms quantify the normalized occupancy of fluorescent regions at the cell periphery (mean ± standard deviation [SD]; 30 < n < 65). Error bars represent 2 × SD. 0.001 < *p < 0.005 and **p < < 0.001, in comparison to wild-type (WT) from two-tailed Student's t test.

(D) Scanning confocal micrographs of GFP-AHDL at cell center (left) and cell periphery (right) in wild-type and *try*Δ cells. Arrows indicate endoplasmic reticulum (ER) breaks at the cortex. Arrowhead indicates an irregular cortical accumulation of ER membranes.

(E) Deconvolved epifluorescence images of wild-type and *try*Δ spheroplasts expressing GFP-AHDL. Left: cell center; right: cell periphery. Scale bars represent 5 μm.

Mid1p efficiently recruited the actomyosin ring assembly machinery to the cortex in *try*Δ cells, but its abnormally broad distribution caused highly delocalized assembly of actomyosin cables.

Upon careful examination, we observed that, following efflux from the nucleus, Mid1p-GFP localized to cortical sites that were positioned close to, but did not overlap with, ER tubules marked by Tts1p-mCherry (Figure 4A). The Mid1p-GFP signal was largely excluded from ER cisternae marked by Ost1p-mCherry (Figure 4B), and the general ER was visualized by mCherry-AHDL (Figure 4C). Thus, it appeared that Mid1p concentrated in nodes at the plasma membrane in between the ER elements. Interestingly, as Mid1p-GFP nodes compacted into a ring, the initially uniformly distributed ER tubules gathered at the cell equator (Figure 4D). This phenomenon underlies the specific enrichment of the putative tubular ER domains at the future division site (Figure 1A). This also implies that their equatorial accumulation is a consequence of node compaction and should depend on both actomyosin function and Mid1p. Indeed, Tts1p-GFP did not accumulate at the cell equator in cells lacking functional formin Cdc12p [16] (Figure 4E) or the essential myosin II light chain, Cdc4p [17] (data not shown). Furthermore, the Tts1p-positive membranes were not enriched in the vicinity of the abnormal actomyosin structures assembled in *mid1*Δ cells (Figure 4F).

Mid1p is targeted to the cortex through two independent motifs. It further oligomerizes and recruits actomyosin ring components [18, 19]. Thus, Mid1p nodes correspond to higher-order protein assemblies. The cortical drift of Mid1p upon mitotic entry in *try*Δ cells (Figure 3C) indicates a high rate of diffusion of these peripherally attached complexes along the membrane prior to cable compaction. Consistent with this proposition, fluorescence recovery after photobleaching (FRAP) analysis of Mid1p-GFP in early mitotic wild-type cells showed only a limited fluorescence recovery (Figure 4G; 28.5% ± 10.9% within 2 min, n = 15), suggesting that the lateral motion of Mid1p was restricted. On the other hand, Mid1p-GFP fluorescence recovery was significantly higher in early mitotic *try*Δ cells (Figure 4H; 62.5% ± 18.7% within 2 min, n = 21, p < 0.01). The slanting traces of Mid1p-GFP fluorescence in kymographs of the FRAP experiments in *try*Δ cells suggest that the observed fluorescence recovery could be due to movement within the plane of the membrane rather than Mid1p turnover (Figure S3F). Thus, it appears that the cortical ER network maintained by the ER tubulating proteins can impede the lateral movement of Mid1p nodes.

We do not favor the possibility that tubular ER defects trigger ring mispositioning through vesicular trafficking abnormalities.

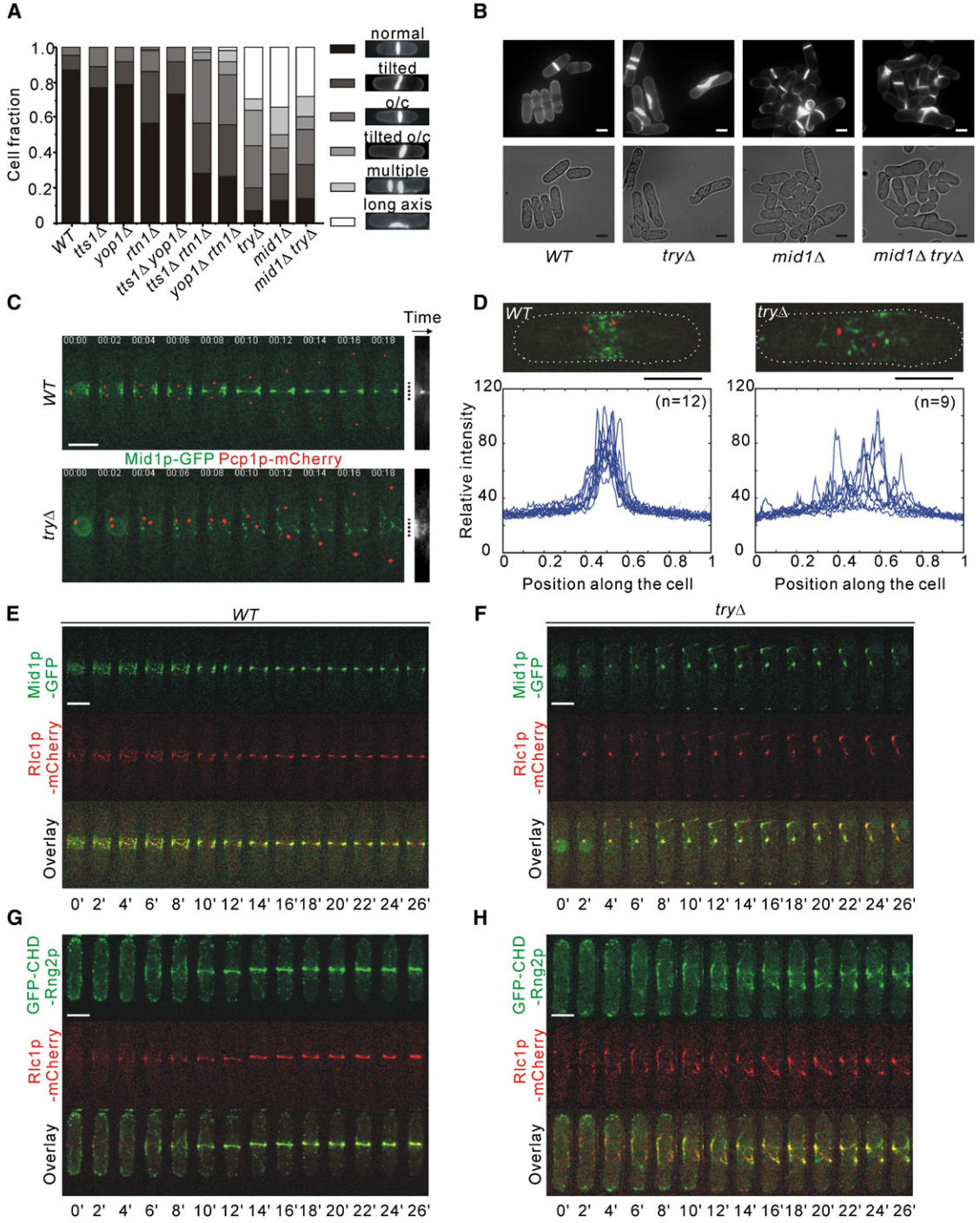

Figure 3. Cells Lacking Rtn1p, Yop1p, and Tts1p Fail to Position and Compact the Actomyosin Ring

(A) Quantification of the septa positioning phenotypes in cells of indicated genotypes (500 < n < 1500). o/c indicates off-center.

(B) Epifluorescence and differential interference contrast images of Calcofluor-stained cells with indicated genotypes.

(C) Time-lapse maximum Z projection images of wild-type and *try*Δ cells coexpressing Mid1p-GFP and Pcp1p-mCherry (left) and corresponding kymographs (right) of Mid1p-GFP along the long cell axis. Dotted lines indicate positions of the nuclei before Mid1p efflux.

(D) Quantification of Mid1p-GFP fluorescence distribution along the long cell axis in wild-type (n = 12) and *try*Δ (n = 9) early mitotic cells, as indicated by Pcp1p-mCherry. Shown are the maximum projections of Z stacks obtained from scanning confocal microscopy.

(E–H) Time-lapse maximum Z projection images of wild-type (E and G) or *try*Δ (F and H) cells coexpressing indicated proteins. Scale bars represent 5 μm. The elapsed time is shown in minutes.

We did not observe defects in transitional ER emergence or Golgi biogenesis in *try*Δ cells (Figure S4). Furthermore, bulk vesicular trafficking deficiencies in *S. pombe* do not lead to ring assembly or positioning defects [20–22]. Concordantly, the lack of reticulons and Yop1p in budding yeast does not cause major secretion defects [3, 6].

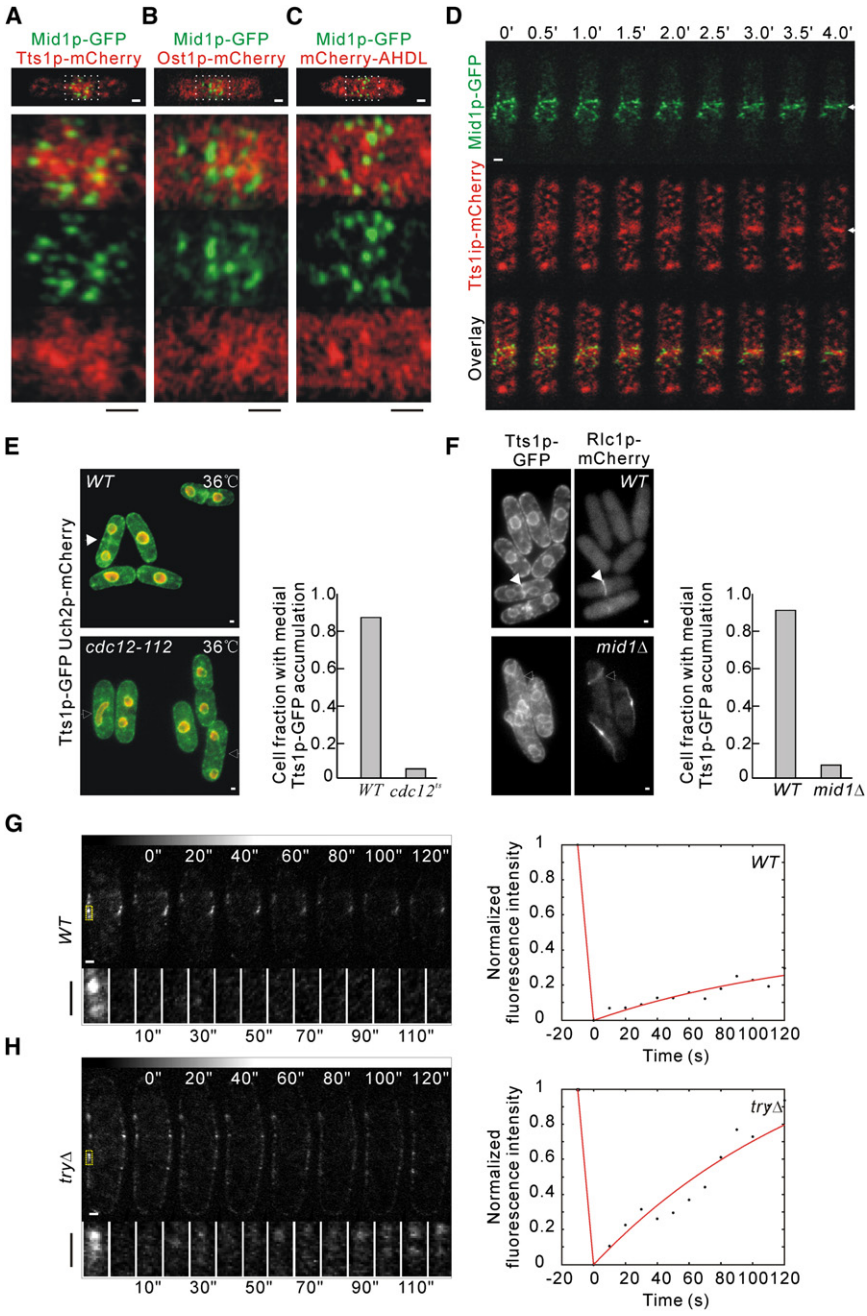

Figure 4. Mid1p Nodes Localize between the Endoplasmic Reticulum Elements during the Actomyosin Ring Compaction

(A–C) Scanning confocal micrographs at peripheral focal plane of wild-type cells coexpressing indicated proteins. Bottom panels show 4× magnification of the framed region.

(D) Time-lapse of early mitotic wild-type cells coexpressing Mid1p-GFP and Tts1p-mCherry imaged by scanning confocal microscopy. Shown is the peripheral focal plane. The arrows indicate the accumulation of Tts1p-mCherry during Mid1p-GFP node compaction. The elapsed time is indicated in minutes.

(E) Localization of Tts1p-GFP (green) in wild-type and *cdc12-112* cells coexpressing Uch2p-mCherry (red) as the nuclear envelope (NE) marker at 36°C. Cells were grown overnight at 24°C and shifted to 36°C for 30 min before imaging. Right: quantification for the medial accumulation of Tts1p-GFP in binucleate cells, n = 100. The solid arrow indicates accumulation of Tts1p-GFP; the outlined arrows indicate lack of the medial accumulation.

(F) Localization of Tts1p-GFP in wild-type (top) and *mid1*Δ (bottom) cells during mitosis, as indicated by Rlc1p-mCherry. Right: quantification for the medial accumulation of Tts1p-GFP in binucleate cells, n = 100. The solid arrows indicate Tts1p-GFP accumulation at the division site; the outlined arrows indicate the disappearance of this accumulation.

(G and H) Mid1p-GFP fluorescence recovery after photobleaching analyses of early mitotic wild-type (G) and *try*Δ (H) cells. Shown are representative cells before and after photobleaching at indicated time points and the corresponding fluorescence recovery curves. Gray wedges at the top show the same contrasting. The bleached regions boxed in yellow are magnified in the bottom rows at all acquired time points. Scale bars represent 1 μm.

The cortical ER in various organisms is intimately associated with the plasma membrane through multiple contact sites [23–27]. One possible outcome of an association between the ER and the cortex is the compartmentalization of their membranes, with their contact sites acting as diffusion barriers for peripherally associated protein complexes. In such a manner, the geometry of the ER network could translate into specific patterning of the plasma membrane and therefore affect the efficiency with which the Mid1p nodes are restricted at the medial cortex. An observed change in node size distribution in *try*Δ cells raises the possibility that, by restricting the spread of Mid1p, the cortical ER network could increase the local concentration of Mid1p and aid its efficient organization into nodes. Furthermore, the ER network could physically hinder the lateral mobility of the nodes, effectively embedding them within the tubular meshwork. Because the physical proximity between neighboring nodes is essential for efficient formation of tight rings [28], broad node distribution would instead lead to assembly of incomplete and mispositioned actomyosin cables. Interestingly, it was previously suggested that Mid1p could be positioned by "as-yet-unidentified structures connecting the nucleus and the cortex" [29]. We propose that the cortical ER network plays an instructive role in delimiting the actomyosin ring assembly at the cell equator.

Similar diffusion-limiting strategies could affect the assembly and function of cortically associated protein networks in other cell types with pronounced ER-plasma membrane attachment sites.

Experimental Procedures

S. pombe Strains, Reagents, and Constructs

S. pombe strains used in this study and their genotypes are listed in Table S1. The promoter and coding sequences for expression of the ER luminal marker GFP-AHDL were introduced at the *leu1* genomic locus with the *S. pombe* integration vector pJK148. GFP-AHDL protein was designed by introducing the signal peptide sequence (25 N-terminal amino

acids) and ER-retention signal (5 C-terminal amino acids) of Bip1p to the N and C termini of the GFP, respectively. Expression of the GFP-AHDL construct was driven by a *bip1* promoter sequence consisting of 1000 bp upstream of the start codon. An identical strategy was used for the mCherry-AHDL construct. Media for vegetative growth and genetic methods were as described in [30]. All experiments were done on cells grown in YES medium. Genetic crosses and sporulation were performed on YPD agar plates. To obtain fission yeast spheroplasts, we grew cells in liquid YES medium overnight to exponential phase and shifted them to a fresh YES medium containing 5 mg/ml Lysing enzyme from Sigma-Aldrich and 3 mg/ml Zymolase (MP Biomedicals) for 90 min to remove the cell wall. The homologous recombination-based method was used to tag endogenous proteins with green fluorescent protein, mCherry, or TAP at their C termini under control of the native promoter. Plasmids were constructed via standard molecular biology techniques. Latrunculin A, a drug that prevents actin polymerization, was purchased from Biomol International LP. DNA fluorescent stain 4′,6-diamidino-2-phenylindole (DAPI) and cell wall stain Calcofluor White were obtained from Sigma-Aldrich. The F-actin stain Alexa Fluor 593 phalloidin was obtained from Invitrogen.

Detailed information on microscopy, image analysis, and biochemical techniques can be found in the Supplemental Experimental Procedures.

Supplemental Information

Supplemental Information includes Supplemental Experimental Procedures, four figures, and one table and can be found with this article online at doi:10.1016/j.cub.2010.04.017.

Acknowledgments

We are grateful to M. Balasubramanian, E. Makeyev, R. Thadani, and S. Cohen for discussions and suggestions on the manuscript. Our work was supported by the Singapore Millennium Foundation.

Received: February 13, 2010
Revised: March 24, 2010
Accepted: April 7, 2010
Published online: April 29, 2010

References

1. Terasaki, M., Jaffe, L.A., Hunnicutt, G.R., and Hammer, J.A., 3rd. (1996). Structural change of the endoplasmic reticulum during fertilization: Evidence for loss of membrane continuity using the green fluorescent protein. Dev. Biol. *179*, 320–328.
2. Voeltz, G.K., Rolls, M.M., and Rapoport, T.A. (2002). Structural organization of the endoplasmic reticulum. EMBO Rep. *3*, 944–950.
3. Voeltz, G.K., Prinz, W.A., Shibata, Y., Rist, J.M., and Rapoport, T.A. (2006). A class of membrane proteins shaping the tubular endoplasmic reticulum. Cell *124*, 573–586.
4. Hu, J., Shibata, Y., Voss, C., Shemesh, T., Li, Z., Coughlin, M., Kozlov, M.M., Rapoport, T.A., and Prinz, W.A. (2008). Membrane proteins of the endoplasmic reticulum induce high-curvature tubules. Science *319*, 1247–1250.
5. Shibata, Y., Voss, C., Rist, J.M., Hu, J., Rapoport, T.A., Prinz, W.A., and Voeltz, G.K. (2008). The reticulon and DP1/Yop1p proteins form immobile oligomers in the tubular endoplasmic reticulum. J. Biol. Chem. *283*, 18892–18904.
6. De Craene, J.O., Coleman, J., Estrada de Martin, P., Pypaert, M., Anderson, S., Yates, J.R., 3rd, Ferro-Novick, S., and Novick, P. (2006). Rtn1p is involved in structuring the cortical endoplasmic reticulum. Mol. Biol. Cell *17*, 3009–3020.
7. West, R.R., Vaisberg, E.V., Ding, R., Nurse, P., and McIntosh, J.R. (1998). cut11(+): A gene required for cell cycle-dependent spindle pole body anchoring in the nuclear envelope and bipolar spindle formation in Schizosaccharomyces pombe. Mol. Biol. Cell *9*, 2839–2855.
8. Vjestica, A., Tang, X.Z., and Oliferenko, S. (2008). The actomyosin ring recruits early secretory compartments to the division site in fission yeast. Mol. Biol. Cell *19*, 1125–1138.
9. Sohrmann, M., Fankhauser, C., Brodbeck, C., and Simanis, V. (1996). The dmf1/mid1 gene is essential for correct positioning of the division septum in fission yeast. Genes Dev. *10*, 2707–2719.
10. Chang, F., Woollard, A., and Nurse, P. (1996). Isolation and characterization of fission yeast mutants defective in the assembly and placement of the contractile actin ring. J. Cell Sci. *109*, 131–142.
11. Bähler, J., Steever, A.B., Wheatley, S., Wang, Y., Pringle, J.R., Gould, K.L., and McCollum, D. (1998). Role of polo kinase and Mid1p in determining the site of cell division in fission yeast. J. Cell Biol. *143*, 1603–1616.
12. Wu, J.Q., Sirotkin, V., Kovar, D.R., Lord, M., Beltzner, C.C., Kuhn, J.R., and Pollard, T.D. (2006). Assembly of the cytokinetic contractile ring from a broad band of nodes in fission yeast. J. Cell Biol. *174*, 391–402.
13. Celton-Morizur, S., Racine, V., Sibarita, J.B., and Paoletti, A. (2006). Pom1 kinase links division plane position to cell polarity by regulating Mid1p cortical distribution. J. Cell Sci. *119*, 4710–4718.
14. Padte, N.N., Martin, S.G., Howard, M., and Chang, F. (2006). The cell-end factor pom1p inhibits mid1p in specification of the cell division plane in fission yeast. Curr. Biol. *16*, 2480–2487.
15. Paoletti, A., and Chang, F. (2000). Analysis of mid1p, a protein required for placement of the cell division site, reveals a link between the nucleus and the cell surface in fission yeast. Mol. Biol. Cell *11*, 2757–2773.
16. Chang, F., Drubin, D., and Nurse, P. (1997). cdc12p, a protein required for cytokinesis in fission yeast, is a component of the cell division ring and interacts with profilin. J. Cell Biol. *137*, 169–182.
17. McCollum, D., Balasubramanian, M.K., Pelcher, L.E., Hemmingsen, S.M., and Gould, K.L. (1995). Schizosaccharomyces pombe cdc4+ gene encodes a novel EF-hand protein essential for cytokinesis. J. Cell Biol. *130*, 651–660.
18. Celton-Morizur, S., Bordes, N., Fraisier, V., Tran, P.T., and Paoletti, A. (2004). C-terminal anchoring of mid1p to membranes stabilizes cytokinetic ring position in early mitosis in fission yeast. Mol. Cell. Biol. *24*, 10621–10635.
19. Almonacid, M., Moseley, J.B., Janvore, J., Mayeux, A., Fraisier, V., Nurse, P., and Paoletti, A. (2009). Spatial control of cytokinesis by Cdr2 kinase and Mid1/anillin nuclear export. Curr. Biol. *19*, 961–966.
20. Poloni, D., and Simanis, V. (2002). A DMSO-sensitive conditional mutant of the fission yeast orthologue of the Saccharomyces cerevisiae SEC13 gene is defective in septation. FEBS Lett. *511*, 85–89.
21. Takegawa, K., Hosomi, A., Iwaki, T., Fujita, Y., Morita, T., and Tanaka, N. (2003). Identification of a SNARE protein required for vacuolar protein transport in Schizosaccharomyces pombe. Biochem. Biophys. Res. Commun. *311*, 77–82.
22. Wang, H., Tang, X., Liu, J., Trautmann, S., Balasundaram, D., McCollum, D., and Balasubramanian, M.K. (2002). The multiprotein exocyst complex is essential for cell separation in Schizosaccharomyces pombe. Mol. Biol. Cell *13*, 515–529.
23. Prinz, W.A., Grzyb, L., Veenhuis, M., Kahana, J.A., Silver, P.A., and Rapoport, T.A. (2000). Mutants affecting the structure of the cortical endoplasmic reticulum in Saccharomyces cerevisiae. J. Cell Biol. *150*, 461–474.
24. Pichler, H., Gaigg, B., Hrastnik, C., Achleitner, G., Kohlwein, S.D., Zellnig, G., Perktold, A., and Daum, G. (2001). A subfraction of the yeast endoplasmic reticulum associates with the plasma membrane and has a high capacity to synthesize lipids. Eur. J. Biochem. *268*, 2351–2361.
25. Sparkes, I.A., Ketelaar, T., de Ruijter, N.C., and Hawes, C. (2009). Grab a Golgi: Laser trapping of Golgi bodies reveals in vivo interactions with the endoplasmic reticulum. Traffic *10*, 567–571.
26. Schneider, M.F. (1994). Control of calcium release in functioning skeletal muscle fibers. Annu. Rev. Physiol. *56*, 463–484.
27. Wu, M.M., Luik, R.M., and Lewis, R.S. (2007). Some assembly required: Constructing the elementary units of store-operated Ca2+ entry. Cell Calcium *42*, 163–172.
28. Vavylonis, D., Wu, J.Q., Hao, S., O'Shaughnessy, B., and Pollard, T.D. (2008). Assembly mechanism of the contractile ring for cytokinesis by fission yeast. Science *319*, 97–100.
29. Daga, R.R., and Chang, F. (2005). Dynamic positioning of the fission yeast cell division plane. Proc. Natl. Acad. Sci. USA *102*, 8228–8232.
30. Moreno, S., Klar, A., and Nurse, P. (1991). Molecular genetic analysis of fission yeast Schizosaccharomyces pombe. Methods Enzymol. *194*, 795–823.